

# Strategic Behavior in Energy and Reserve Co-optimizing T&D Markets with EV Participants: **Long Version with Appendices**

Fatma Selin Yanikara<sup>1</sup>, Evgeniy Goldis<sup>2</sup>, Michael Caramanis<sup>1</sup>

**Abstract**—This paper compares Transmission and Distribution (T&D) network day-ahead market (DAM) algorithms clearing energy and reserves under various cases of information available to either a centralized or distributed decision maker. Flexible Distributed Energy Resource (DER) loads transacting hourly energy and reserves are market participants in addition to conventional generators and inelastic demand. DERs are connected to distribution networks where line losses are significantly higher than in the high voltage transmission network. Distributed-algorithm-based Market clearing with self-scheduling DERs is required for computation and information communication tractability. Under certain conditions of information available to flexible DER loads, strategic behavior is possible. This paper’s contribution is the investigation of the likelihood and severity of DER strategic behavior. It investigates the Nash Equilibrium achieved by self-scheduling of profit maximizing DER-market-participants adapting iteratively to hourly day-ahead energy and reserve marginal-cost-based prices set by collaborating T&D Independent System Operators. The Nash Equilibria obtained under different cases of distribution network information available to individual DERs or their aggregator are compared to social welfare maximizing DER schedules obtained by an “all knowing” Centralized Market Operator (CMO). Comparison of Nash and Social Welfare maximizing Equilibria across the aforementioned information availability cases, indicates that under some -- possibly impractical -- information availability cases, self-scheduling DERs can achieve a higher profit than under a social welfare maximizing CMO, a result magnified by DER collusion through an aggregator. We perform numerical experiments on a simple T&D network modeling salient characteristics of EV mobility, battery electrochemistry charging constraints and distribution network losses.

## I. INTRODUCTION

Increasing penetration of environmentally sustainable, albeit intermittent and volatile, renewable generation can benefit handsomely from significantly positive synergies with equally increasing storage-like flexible Distributed Energy Resource (DER) loads. DERs, supreme among them electric vehicles (EVs), can schedule their hourly charging capacity to charge their battery and promise secondary reserves. EVs self-schedule by maximizing their benefits while adapting iteratively to hourly day-ahead distribution location marginal-cost-based prices (DLMPs) determined by collaborating T&D Independent System Operators. Note that DLMPs are equal to transmission locational marginal prices (LMPs) adjusted for distribution line marginal loss and other distribution network marginal costs [14]. Unfortunately, familiar centralized market

clearing algorithms administered by a Centralized Market Operator (CMO) with access to T&D network as well as T&D connected participant preferences are intractable. The reason is that DERs connected to medium/low voltage distribution networks are much more numerous than conventional generators, and possess intertemporal and complex preferences and capabilities. Load aggregation and direct centralized utility control methods proposed in the literature in order to address these difficulties [1-3] as well as open-loop optimal EV charging approaches [10,15] are not scalable for DER market integration. Distributed algorithm methods based on DER self-scheduling that adapts to DLMPs determined by a single T&D Independent System Operator (T&DISO) or collaborating Transmission and Distribution Independent System Operators (TISO), (DISO) is the only tractable approach to the complex DER preferences and dynamics and the associated information communication constraints [8, 14].

Given the unavoidable self-scheduling of DERs under tractable distributed-algorithm-based market clearing approaches, two important questions arise: (i) Is there a unique and reasonably fast converging Nash Equilibrium that can be obtained for the market to clear, and moreover, (ii) are there opportunities for DERs to engage in strategic behavior enabling them to increase their individual benefits at the expense of social welfare? Needless to mention that there is a vast literature on these topics. To mention a few, the reader is referred to [16] and [20] on the theory of the existence of Nash Equilibrium in well behaved (convex) markets and [5, 7, 9, 11, 18, 21] for convergence and strategic behavior issues. It is the second question that we address in this paper and this constitutes the paper’s contribution.

This paper contributes to past work by investigating cases of network-information-access enabling social welfare compromising DER strategic behavior. Furthermore, it sheds light on the feasibility of accessing such information, the magnitude of the associated loss of social welfare, and, finally, market design/regulatory options that can mitigate DER strategic behavior.

We are able to obtain analytical as well as extensive numerical results by (i) focusing on EV DERs and modeling their day ahead market dynamics at a high level of fidelity by considering actual battery dynamics [17] and mobility, and (ii) modeling accurately centralized generator costs and capabilities but simplifying, albeit without loss of generality as regards our analytical results, the transmission and distribution networks. Although a CMO is not tractable for realistic size problems, we are able to formulate its model for the simplified

<sup>1</sup>Boston University, Division of Systems Engineering. [yanikara@bu.edu](mailto:yanikara@bu.edu)

<sup>2</sup>Newton Energy Group

transmission and distribution network representation and solve it for small problem instances so that the optimal social welfare can be quantified and compared to the outcome of distributed decision making. More importantly, analytic expressions of market equilibrium optimality conditions under a CMO can be compared to the conditions under distributed market clearing Nash Equilibria corresponding to the various network information access cases considered. Distributed market clearing information cases include (i) D: Individual DERs respond to day ahead hourly DLMPs as pure price takers; they do not know (nor can they learn) how their decisions may affect DLMPs or the decisions of other DERs, (ii) D<sub>N</sub>: Individual DERs know the relevant LMPs and can map them to the DLMPs by estimating the marginal losses at their location. (iii) D<sub>A</sub>: DERs assign their scheduling to an aggregator who knows the decision of all DERs, but does not know marginal losses (iv) D<sub>N,A</sub>: as above, except that the aggregator knows marginal losses.

The main conclusion of the paper is that whereas there is no social welfare compromise under D and D<sub>A</sub>, strategic behavior is possible and of increasing importance as we move to cases D<sub>N</sub> and D<sub>N,A</sub>. A non-surprising conclusion is that aggregation or collusion amongst DERs is prima face undesirable. In addition, we can argue that cases D<sub>N</sub> and D<sub>N,A</sub> are equivalent to allowing the Distribution Independent System Operator (DISO) to serve as an Energy Service Company (ESCO) that schedules all EVs. Should this be allowed for the *independent* DSO? Would it be necessary to have aggregating ESCOs if information platforms allowing individual EV scheduling become available?

The remainder of this paper is organized as follows: Section II presents a simplified model of a meshed and lossless Transmission network connected to Distribution Feeders with explicit non-linear line losses; conventional price inelastic loads and price elastic EVs are connected to the Distribution network, while conventional generators are connected to the Transmission network. Different cases of distribution network information available the ISO and to EVs are defined. Section III presents the EV battery model, distributed day ahead market (DAM) clearing model constituting an iterative DER-T&DISO hierarchical game: individual EVs self-schedule against forward T&DISO DLMP estimates. DERs reschedule till a Nash Equilibrium is achieved at a reasonable convergence rate associated with adaptive DLMP update conditions. In addition, EVs have the option to either self-schedule or entrust their schedules to a load aggregator ESCO. Section IV presents two CMO algorithm versions. In version C the CMO has access to EV preferences and collaborates with the DISO to translate LMPs to DLMPs. In version C<sub>N</sub>, the CMO has access to EV preferences and also to all DISO network information. Under version C<sub>N</sub>, the CMO clears the market achieving the maximal social welfare in a single iteration, while a few iterations are needed in the C version of the CMO. Section V represents the differences in the optimality conditions that characterize the centralized and distributed algorithms under various distribution network information availability and load aggregation options. Section VI presents numerical results and Section VII concludes.

Notation	Definition
<i>Indices and sets</i>	
$n, n(i), j$	Transmission bus $n$ ; associated Distribution feeder bus $n(i), i \in S_{n(i)}$ ; EV $j$
$S_n, S_{n(i)}, S_{n(i)}^j, H, H^j$	Set of transmission buses, Set of feeders that belong to transmission bus $n$ , Set of feeders EV $j$ visits, set of hours, set of hours that EV $j$ is mobile/traveling; $H^j \subset H$ .
$h, h_{j,n(i)}^a, h_{j,n(i)}^d$	Hour $h \in H$ ; arrival/depart. hour of EV $j$ to/from $n(i)$ . $h = 0..24$
$\Gamma_h(i, j), i(j, h), i^*$	Location assignment matrix of EV $j$ . $\Gamma_h(i, j) = 1$ if EV $j$ is in feeder $i$ at time $h$ , location of EV $j$ at time $h$ , $i^* = i(j, h)$ s.t. $\Gamma_h(i^*, j) = 1$
<i>EV variables and parameters</i>	
$p_h^j, r_h^j$	Real power (p) consumed and reserves provided (r) by EV $j$ during hour $h$
$\{a_h^j, b_h^j\}, x_h^j$	KiBaM battery state of charge (SoC) variables, Total battery SoC of EV $j$ at the beginning of hour $h$ . Note that $x_h^j = b_h^j + a_h^j$
$\bar{u}_h^j(b_h^j, a_h^j), \bar{C}^j, \bar{P}$	Max charging rate function, Energy Storage capacity of EV $j$ , rated power of the outlet
$U(a_{h_{n(i)}^d}^j + b_{h_{n(i)}^d}^j)$	Quadratic cost/disutility of EV $j$ when total SoC $< \bar{C}_{n(i)}^j$ when it departs $n(i)$ . $U(a_{h_{n(i)}^d}^j + b_{h_{n(i)}^d}^j) = \gamma(\bar{C}^j - (b_{h_{n(i)}^d}^j + a_{h_{n(i)}^d}^j))^2$
$S_h^j$	Energy spent by EV $j$ during traveling at hour $h$ ; $h \in H^j$ .
<i>Generator variables and parameters</i>	
$p_h^g, r_h^g$	Real power (p) generated and reserves provided (r) by generator $g$ during hour $h$
$\bar{g}, g$	Generator $g$ capacity and technical minimum
$\bar{c}^g(p_h^g), \bar{r}^g(r_h^g)$	Convex cost of energy and reserve provision respectively of generator $g$
<i>Network and system parameters</i>	
$d_h^{n(i)}, R_h$	Conventional/inelastic demand at $n(i)$ ; system reserve requirement at hour $h$
$L_h^{n(i)}, m_h^{n(i)}$	Total and marginal Losses over distribution feeder connecting busses $n$ and $n(i)$
$\lambda_h^n, \rho_h$	Ex-Post Marginal Cost of energy and reserves at transmission bus $n$ (i.e., LMP <sup>E</sup> and LMP <sup>R</sup> )
$\lambda_h^{n(i)}, \rho_h^{n(i)}$	Ex-Post Marginal Cost of energy and reserves at distribution bus $n(i)$ (i.e., DLMP <sup>E</sup> and DLMP <sup>R</sup> )

Acronyms	
DAM	Day ahead Market
DER, EV	Distributed Energy Resource, Electric Vehicle
TISO, DISO, T&DISO, CMO	Transmission Independent System Operator, Distribution Ind. System Operator, T&D Ind. System Operator, Central Market Operator
D, D <sub>A</sub> , D <sub>N</sub> , D <sub>N,A</sub> , C, C <sub>N</sub>	Cases of distributed (D) and centralized (C) models. See Section I for definitions.
KiBaM	Kinetic Battery Model

## II. T&D NETWORK APPROXIMATION AND CASES OF INFORMATION AVAILABILITY

Following the above notation definition we formulate a stylized T&D network consisting of a meshed High Voltage finite line capacity but lossless transmission Network with nodes  $n$ , and loss-incurring distribution feeders, each represented by a single line  $n, n(i)$  as shown in Figure 1. Feeder demand is aggregated at each  $n(i)$  and equals the sum of inelastic conventional demand and EVs connected at the distribution side of each feeder. Conventional centralized generators are connected to transmission side nodes  $n$ . More realistic renditions of the T&D Network (see for example [14]) do not affect our results. We assume quadratic losses over distribution feeders and define the details of the aforementioned information access next:

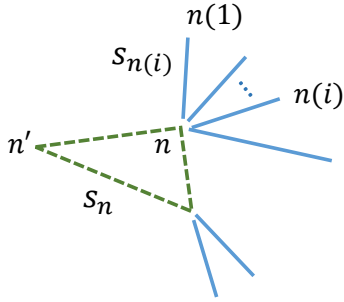


Figure 1. T&D Network approximation

### A. Distribution Network Information

Assuming quadratic distribution feeder losses, we write

$$L_h^{n(i)} = \frac{\beta^{n(i)}}{2} (d_h^{n(i)} + \sum_{j|\Gamma_h(i,j)=1} p_h^j)^2 = \frac{\beta^{n(i)}}{2} (\ell_h^{n(i)})^2$$

where  $\beta^{n(i)}$  is the ratio of line resistance over the square of voltage at bus  $n(i)$ . Marginal losses of additional load at  $n(i)$  are  $m_h^{n(i)} = \beta^{n(i)} \ell_h^{n(i)}$ . Distributed loads at feeder  $n(i)$  and the resulting withdrawal at node  $n$  are:

$$\ell_h^{n(i)} = d_h^{n(i)} + \sum_{j|\Gamma_h(i,j)=1} p_h^j$$

$$\ell_h^n = \sum_{i \in S_n(i)} (\ell_h^{n(i)} + L_h^{n(i)})$$

Similarly, distributed reserve offers,  $r_h^{n(i)}$ , and the resulting reserves that can be delivered upon deployment<sup>1</sup> to transmission node  $n$  are:

$$r_h^{n(i)} = \sum_{j|\Gamma_h(i,j)=1} r_h^j$$

$$r_h^n = (1 + m_h^{n(i)}) \sum_{i \in S_n(i)} r_h^{n(i)}$$

We finally note that spatiotemporal real power and reserve marginal costs at node  $n$ , ( $LMP^E$ ,  $LMP^R$ ), and at feeder  $n(i)$ , ( $DLMP^E$ ,  $DLMP^R$ ), are related by

$$\lambda_h^{n(i)} = (1 + m_h^{n(i)}) \lambda_h^n \quad \text{and} \quad \rho_h^{n(i)} = (1 + m_h^{n(i)}) \rho_h^n$$

Readers interested in the detailed physics of distribution networks, should note that our single distribution line representation of distribution feeders with all distribution feeder loads and DERs connected to a single node constitute an approximation/aggregation that subsumes dynamically changing radial feeder topologies and locational load distribution. As a result, the effort that EV  $j$  would have to undertake to know in a real feeder the equivalent of  $\beta^{n(i)}$  and total load of other customers,  $\ell_h^j$ , is far from negligible.

### B. Cases of Information Available to DERs in the Iterative Distributed-Algorithm-Market-Clearing Model

During iteration  $k$ , each EV schedules and optimally allocates its capacity between  $p_h^{j,k+1}$  and  $r_h^{j,k+1}$ ,  $\forall h$  so as to maximize its utility of a charged battery at the time of departure minus the cost of power purchased plus the income from providing regulation service reserves subject to constraints. As shown in Section III, each EV  $j$  solves in iteration  $k$ , an optimization problem that depends on its knowledge about  $\lambda_h^{n(i),k}$  and  $\rho_h^{n(i),k}$ ,  $\forall h$ . The two information cases of the distributed algorithm we consider are (i) without access to information about feeder losses and complementary loads, and (ii) full access to feeder losses and complementary loads. These cases are detailed below:

#### Case D - Distributed algorithm with no feeder information:

DLMP estimates  $\hat{\lambda}_h^{n(i),k}$  and  $\hat{\rho}_h^{n(i),k}$   $\forall h$  are provided at the beginning of iteration  $k$  by the Transmission Independent System Operator (TISO) in collaboration with the Distribution Independent System Operator (DISO). TISO schedules centralized generation connected to Transmission nodes  $n$ , conditional upon self-scheduled EV quantities at the most recent iteration,  $p_h^{j,k}, r_h^{j,k}$   $\forall h, j$ . The resulting DLMPs can be

<sup>1</sup> We assume that incremental losses at full reserve deployment are adequately represented by marginal losses.

interpreted as ex-post DLMPs and are used to determine DLMP estimates  $\hat{\lambda}_h^{n(i),k}$  and  $\hat{\rho}_h^{n(i),k} \forall h$  in a manner that assures convergence of the iterative algorithm as described in the TISO problem of Section III.

**Case D<sub>N</sub> - Distributed algorithm with full feeder information:**

LMP estimates  $\hat{\lambda}_h^{n,k}$  and  $\hat{\rho}_h^k, \forall h$  are provided at the beginning of iteration  $k$  by the TISO on the basis of ex-post LMPs derived in a manner similar to the one above. Loss information  $\beta^{n(i)}$ , and the complementary load to EV  $j$  at feeder  $n(i)$ , denoted by  $\ell_h^{\bar{j},n(i),k}, \forall h$  as well as the closed form expression for losses is provided by the DISO. The complementary load to EV  $j$  is expressed as:

$$\ell_h^{\bar{j},n(i)} = d_h^{n(i)} + \sum_{j|\Gamma_h(i,j)=1, j' \neq j} p_h^{j'}$$

We can therefore write the DLMPs as a function of the individual EV decisions,

$$(i) \hat{\lambda}_h^{n(i),k} = (1 + \beta^{n(i)} (\ell_h^{\bar{j},n(i)} + p_h^{j,k+1})) \hat{\lambda}_h^{n,k}$$

$$(ii) \hat{\rho}_h^{n(i),k} = (1 + \beta^{n(i)} (\ell_h^{\bar{j},n(i)} + p_h^{j,k+1})) \hat{\rho}_h^k$$

Knowledge of complementary loads changes the properties of the optimization problem that each EV solves. The distributed algorithm represents a first step of EVs connected to the same feeder toward colluding by sharing charging decisions. The next step that completes the collusion is to rely on an aggregator/ ESCO to schedule all EVs.

**Cases D<sub>A</sub> and D<sub>N,A</sub>:** Similar to the cases above, except that all EVs connected to a substation are scheduled by a *load aggregator* (A) who determines  $p_h^j, r_h^j \forall h, j$ . Note that in case D<sub>N,A</sub> the load aggregator can relate its DLMP to the LMP since it has access to the following information:

$$(i) \hat{\lambda}_h^{n(i),k} = (1 + \beta^{n(i)} (d_h^{n(i)} + \sum_{j|\Gamma_h(i,j)=1} p_h^{j,k+1})) \hat{\lambda}_h^{n,k}$$

$$(ii) \hat{\rho}_h^{n(i),k} = (1 + \beta^{n(i)} (d_h^{n(i)} + \sum_{j|\Gamma_h(i,j)=1} p_h^{j,k+1})) \hat{\rho}_h^k$$

**C. Cases of Information Available to Centralized-Algorithm-Market-Clearing**

The centralized market clearing algorithm utilizes full information of the intertemporal preferences and capabilities of EVs, and simultaneously schedules centralized generator and EV energy and reserve decisions including  $P_h^g, r_h^g, P_h^j, r_h^j, \forall h$ . Besides full EV information, the CMO may have all of the TISO and DISO information or have to rely on a separate DISO entity to provide loss and marginal loss information. The two resulting CMO versions are described below.

**Case C – CMO has partial information on the network losses:** The CMO schedules centralized generation and EVs with partial distribution network information limited to feeder

losses and marginal losses,  $\hat{L}_h^{n(i)}, \hat{m}_h^{n(i)} \forall h$ , provided by the DISO, conditional upon the tentative schedules of  $p_h^j, r_h^j, \forall h$ . This may be desirable or cost effective to avoid communication delays between the multitude of DISOs managing  $\sim |s_{n(i)}| |s_n|$  feeders, and the CMO. In addition, real feeders are not a simple aggregate distribution line and may be subject to topology changes (see for example [14]). This requires few iterations between the CMO and the DISOs to converge. The resulting schedules can be considered a second best to the socially optimal equilibrium obtained by the full information case described below.

**Case C<sub>N</sub> – CMO has full information on network characteristics and losses:** The CMO has perfect information about distribution feeder topology and electrical properties so that location specific losses can be expressed in terms of the decision variables. CMO is therefore an entity that combines TISO and all DISO information, has access to all DER details, hence can clear the market and maximize social welfare in one step. The optimality conditions of Case C<sub>N</sub> characterize the socially optimal equilibrium to which we compare all other distributed algorithm based information access cases.

**III. ITERATIVE DISTRIBUTED MARKET CLEARING ALGORITHM**

The individual EV and the TISO/DISO problems mentioned in Section II are presented here in more detail along with the battery electrochemistry constraints model. Recall that at each iteration  $k$  of the distributed model, (i) all EVs solve for their optimal schedules by adapting to T&DISO provided DLMP estimates, and (ii) the TISO optimizes centralized generation schedules conditional upon feeder loads and reserve offers determined by EV sub-problem solutions, and finally (iii) updated DLMP or LMP estimates (in cases D<sub>N</sub> and D<sub>N,A</sub>) are provided to each feeder bus  $n(i)$ , in order to proceed to iteration  $k + 1$ . The battery model, the EV sub-problems and the TISO generation optimization steps showing dual variables associated with constraints are presented next.

**Battery model:**

The battery is represented as a two bucket system, based on the Kinetic Battery Model in [17] adapted for the charging phase and normalized in terms of units of power. Total charge is modeled as the sum of energy charged in two buckets. Power directly flows into the second bucket ( $b$ ) and from there it is transferred to the first bucket ( $a$ ) at a rate proportional to the charge difference w.r.t. bucket  $b$  (see Figure 2). The following time differential equations represent the battery charging dynamics with  $h \leq t \leq h + 1$  the continuous time evolution during hour  $h$ :

$$\dot{b}_t^j = [1 - \varepsilon p_t^j] p_t^j - \kappa (b_t^j - a_t^j)$$

$$[1 - \varepsilon p_t^j] p_t^j \text{ unconstrained for } b_t^j < \bar{b}^j$$

$$[1 - \varepsilon p_t^j] p_t^j \leq \kappa (b_t^j - a_t^j) \text{ for } b_t^j = \bar{b}^j \text{ (KiBaM.1)}$$

$$\dot{a}_t^j = \kappa (b_t^j - a_t^j) \text{ (KiBaM.2)}$$

The differential equations can easily provide the maximum constant charging rate that is sustainable during hour  $h$  as a function of the level of the first and second bucket at the beginning of hour  $h$ , which we denote by  $\bar{u}_h^j(a_h^j, b_h^j)$ . This model captures the underlying idea that the maximal constant hourly charging rate is constrained by the bucket specific SoC at the beginning of the hour.

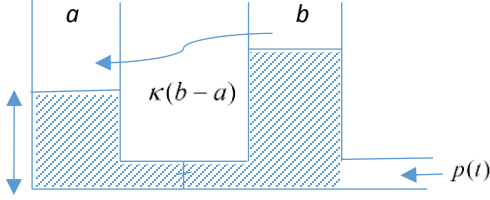


**Figure 2** - Illustration of the two-bucket Kinetic Battery Model (KiBaM).  $\kappa$  is the constant transfer rate between bucket  $b$  and  $a$ .

### EV problem for EV $j$ – Case D:

$$\min_{p_h^{j,k+1}, r_h^{j,k+1}} \sum_h (\hat{\lambda}_h^{n(i^*),k}) p_h^{j,k+1} - (\hat{\rho}_h^{n(i^*),k}) r_h^{j,k+1} + \sum_{n(i) \in s_n^j} U(a_{h(n)}^j + b_{h(n)}^j) \quad (\text{EV.1})$$

s.t

$$i^* = \{i \mid \Gamma_h(i, j) = 1\}$$

$$b_h^j = f(b_{h-1}^j, a_{h-1}^j, \mathbf{1}_{h \notin H^j} p_{h-1}^j, \mathbf{1}_{h \in H^j} S_{h-1}^j) \rightarrow v_h^{j,k+1}$$

$$a_h^j = g(b_{h-1}^j, a_{h-1}^j, \mathbf{1}_{h \notin H^j} p_{h-1}^j, \mathbf{1}_{h \in H^j} S_{h-1}^j) \rightarrow \alpha_h^{j,k+1} \quad (\text{EV.2})$$

$$p_h^j \leq \min \{ \bar{P}, \bar{u}_h(a_h^j, b_h^j) \} + \varepsilon (\bar{u}_h(a_h^j, b_h^j))^2 \rightarrow \zeta_h^{j,k+1} \quad (\text{EV.3})$$

$$r_h^j \leq \min \{ p_h^j, \bar{P} - p_h^j, 0.8 \bar{u}_h(a_h^j, b_h^j) \} \rightarrow \delta_h^{j,k+1} \quad (\text{EV.4})$$

$$b_h^j \leq \bar{b}, \quad a_h^j \leq \bar{a} \rightarrow \varrho_h^{j,k+1} \quad (\text{EV.5})$$

$\hat{\lambda}_h^{n(i),k}, \hat{\rho}_h^{n(i),k}$  determined by Section II.B relations

that apply to Case D,  $D_A$  or  $D_N, D_{N,A}$ . For cases  $D_A$  and  $D_{N,A}$  decisions include  $\forall j$  connected to the same bus  $n$  and the objective function is augmented by summing over  $\forall h, \forall n(i) \in s_{n(i)}, \forall j \in \{j \mid \Gamma_h(n(i), j) = 1\}$ , where the constraints (EV.2-5) are also for  $\forall j$ .

Note that the objective function (EV.1) represents charging cost net of reserve revenue and disutility of battery SoC, (EV.2) shows the intertemporal SoC dynamics in terms of the constant charging rate during hour  $h$ , with functions  $f$  and  $g$  obtained from the solution of battery differential equations that incorporate also the impact of energy expended if the EV is traveling during an hour. (EV.3) includes a quadratic efficiency term expressing losses in the conversion of outlet drawn power rate to battery stored energy. Inequality constraint EV.4 represent the requirements of up and down secondary reserves considered here (for details see [10, 15]).

EV.4 also captures the limits on the maximum amount of reserves promised by the EV, considering the real-time tracking of the regulation signal. An EV that promises reserves equal to the maximum charging rate may not be able to track the signal reasonably well when the second bucket,  $b$ , reaches its capacity. Therefore, a conservative upper bound is adopted. Figure 3 shows an example case where in the beginning of the hour an EV is able to track the regulation signal rebroadcasted by the TISO during the hour in 2 second intervals. However, as the SoC increases, most probably for  $t$  close to  $h+1$ ,  $b_t^j$  reaches its capacity  $\bar{b}_t^j$  forcing  $p_t^j$  to plunge to  $[1 - \varepsilon p_t^j] p_t^j = \kappa(b_t^j - a_t^j)$  which may fall short of the level required by the regulation signal  $y_t$ , cause the tracking error to skyrocket and disqualify the EV from participating in the reserves market. Finally, EV.5 ensures that battery SoC is within the capacity limit. For simplicity we let  $\bar{a}^j = \bar{b}^j = \bar{C}^j/2$ .

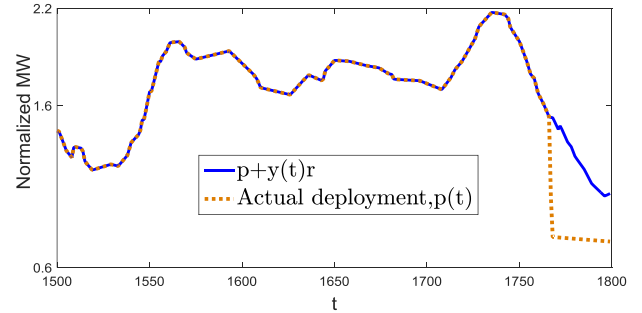


**Figure 3** - Differences in the actual deployment and zero tracking error consumption of EV  $j$  in real time. The actual deployment may fall short of the regulation signal  $y(t)$  resulting in high tracking errors.

### TISO problem determining optimal schedules of $p_h^{g,k+1}, r_h^{g,k+1}$

$$\min_{p_h^{g,k+1}, r_h^{g,k+1}} \sum_{g,h} [\bar{c}^g (p_h^{g,k+1}) + \bar{r}^g (r_h^{g,k+1})] \quad (\text{TISO.1})$$

s.t

• *Energy and reserve balance constraints:*

$$\sum_g p_h^{g,k+1} - \sum_{n(i)} (\ell_h^{n(i),k+1} + L_h^{n(i),k+1}) = 0 \rightarrow \lambda_h^{k+1} \quad (\text{TISO.2})$$

$$\sum_g r_h^{g,k+1} + \sum_{n(i), j \mid \Gamma_h(i,j)=1} (1 + m_h^{n(i),k+1}) r_h^{j,k+1} \geq R_h \rightarrow \rho_h^{k+1} \quad (\text{TISO.3})$$

• *Generator capacity constraints:*

$$p_h^g - r_h^g \geq \underline{g} \rightarrow \zeta_h^{g,k+1} \quad (\text{TISO.4})$$

$$p_h^g + r_h^g \leq \bar{g} \rightarrow \xi_h^{g,k+1}$$

With  $L_h^{n(i),k+1}$  and  $m_h^{n(i),k+1}$  dependent on iteration  $k+1$  EV decisions consistent with Section II A relations.

Recall that the TISO problem optimizes centralized generation schedules conditional upon given EV schedules. The objective function (TISO.1) represents the energy generation and reserve provision cost of centralized generators. Equations (TISO.2-3) represent the energy balance and reserve constraints resulting in shadow prices  $\lambda_h^n$  and  $\rho_h$ , respectively. For ease of exposition we consider a simplified version of the Transmission network where line flow capacity constraints are never binding, rendering  $\lambda_h^n = \lambda_h \forall n$ . (TISO.4) represents centralized generator capacity constraints. We note that EV schedule convergence may be slowed by synchronization effects causing EV energy consumption to oscillate across two hours in response to also oscillating DLMPs. Adaptive price update rules (see Appendix A.3) and strict convexity (e.g. quadratic charging efficiency) are crucial in mitigating convergence problems.

#### IV. CENTRALIZED MARKET CLEARING MODEL

The centralized market clearing problem solved by the CMO is written as:

$$\begin{aligned} & \min_{p_h^g, r_h^g, p_h^j, r_h^j} \sum_{g,h} [\bar{c}^g(p_h^g) + \bar{r}^g(r_h^g)] \\ & + \sum_{n(i) \in S_{n(i)}^j} U(a_{h_{m(i)}}^j + b_{h_{m(i)}}^j) \quad (\text{CMO.1}) \\ & \text{subject to:} \\ & \bullet \text{ Energy and reserve balance constraints} \\ & \sum_g p_h^g - \sum_{n(i)} \ell_h^{n(i)} - L_h^{n(i)} = 0, \forall h \rightarrow \lambda_h \quad (\text{CMO.2}) \\ & \sum_g r_h^g + \sum_{n(i), j | \Gamma_h(i,j)=1} (1 + m_h^{n(i)}) r_h^j \geq R_h, \forall h \rightarrow \rho_h \quad (\text{CMO.3}) \\ & m_h^{n(i)}, L_h^{n(i)} \text{ determined using Section II.C relations} \\ & \text{depending on whether case C or } C_N \text{ applies.} \\ & \bullet \text{ Generation capacity constraints (TISO.4)} \\ & \bullet \text{ EV state dynamics and constraints (EV 2-5)} \end{aligned}$$

Note that in version  $C_N$  the market clears in one step, whereas version C requires a few iterations between the CMO who has access to DER preference and TISO network information with the DISO who collaborates to provide total substation loss and marginal feeder specific loss estimates.

#### V. OPTIMALITY MISMATCH BETWEEN VARIOUS INFORMATION AVAILABILITY CASES

Equilibrium conditions for each of the four distributed, and the two CMO problems can be obtained by forming the Lagrangians of all sub-problem in each distributed algorithm information access sub-problem (a single problem in the CMO cases), and setting gradients with respect to decision variables to zero [16, 21]. Careful analysis and comparison of equilibrium conditions (see Appendix A.2) show mismatches in the conditions summarized in Table 1. For notational simplicity, mismatches are shown for a single transmission node and a single distribution feeder; and the time arguments

are not included. Generalization is possible with salient characteristics and conclusions remain unchanged. Distribution and transmission location designations are also omitted as they can be surmised by the presence of loads (distribution) or generators (transmission).

**Table 1-** Pair wise comparison of optimality conditions with energy and reserves.

	C	$C_N$
D	None	$-\beta \rho_{C_N} \sum_j r_{C_N}^j$
$D_A$	None	$-\beta \rho_{C_N} \sum_j r_{C_N}^j$
$D_N$	$\beta(\rho_{D_N} r_{D_N}^j - \lambda_{D_N} p_{D_N}^j)$	$\beta(-\rho_{C_N} \sum_{j \neq j} r_{C_N}^j - \lambda_{D_N} p_{D_N}^j)$
$D_{N,A}$	$\beta(\sum_j \rho_{D_{N,A}} r_{D_{N,A}}^j - \lambda_{D_{N,A}} p_{D_{N,A}}^j)$	$-\beta \lambda^{D_{N,A}} \sum_j p^{j,D_{N,A}}$

Differences in the optimality conditions imply differences in the primal decisions and therefore also in the dual variables, i.e.,  $\lambda_h$ ,  $\rho_h$ ,  $\lambda_h^{n(i)}$  and  $\rho_h^{n(i)}$ , as well as dual variables associated with constraints EV.2-4. In addition, by inspection of the equilibrium condition differences, we observe that optimality condition differences approach 0 as the energy consumed and the reserves offered by an EV/DER approach zero, and as the distribution network capacity is enhanced resulting in a smaller loss coefficient,  $\beta$ , magnitude.

It is also noteworthy that comparison of C with  $D_A$ , or C with D, shows that when neither the centralized decision maker nor the DERs (or their aggregator) have access to distribution network information, -- i.e. when a DSO acts as an intermediate who translates LMPs to DLMPs and estimates losses -- strategic DER behavior is not effective! To be precise, in the absence of access to distribution network information, the Nash Equilibrium reached by the distributed-algorithm is identical to the centralized-algorithm reached equilibrium, and, as such, case C achieves a stable market clearing equilibrium. On the other hand, when DERs have access to distribution network information, they can lower their effective cost by engaging in strategic behavior and self-schedule in ways that differ the social welfare maximizing DER schedules derived by  $C_N$ . In other words, the CMO equilibrium is unstable when DERs have access to network information.

Analyzing further Table 1, we note opposite signs in the mismatch terms between C and  $C_N$  relative to  $D_{N,A}$  or  $D_N$ . Under asymmetric access to information between DERs and CMO, DER self-scheduling deviates more from the  $C_N$  equilibrium than they do from the C equilibrium schedule. In other words, the DER incentives to differ from the C equilibrium are smaller than the incentives to differ from the  $C_N$  equilibrium. Indeed, noting that  $\sum r_h^j \leq \sum p_h^j$  from relation (EV.4), and the reasonable assumption that  $\lambda_h \sim \rho_h$ , we conclude that the deviation between C and  $D_N$  is smaller than the deviation between  $C_N$  and  $D_N$ .

The analytical results in Table 1 are reinforced by the numerical results reported in Table 2 which imply that the largest deviation from the social optimum achieved by DER strategic behavior occurs when DERs have access to distribution network information while the CMO also has distribution network information ( $C_N$ ). Recalling that information constraints render  $C_N$  intractable for real size problems, we argue that the market equilibrium under CMO version C, is not only identical to the distributed algorithm equilibrium under cases D and  $D_A$ , but is also very close to the equilibrium under case  $D_N$  or  $D_{N,A}$ .  $D_{N,A}$  is in fact a market rendition where the DISO acts as a load aggregator with full access to Distribution Network information.

## VI. NUMERICAL RESULTS

Numerical results are reported and discussed here to illustrate the differences between Socially Optimal/CMO and Distributed Algorithm market clearing under various information access cases. We model a three feeder distribution network with six categories of EVs traveling between two feeders with different plug in/arrival and departure times, 24 kWh batteries, a 7.2 kW charger, overall charging demand  $\sim 1.4\%$  of the conventional loads and system reserve requirements at 6% of conventional demand. Centralized generators have continuous quadratic energy and reserve supply costs, and there is no Transmission congestion. EVs in the same group share identical characteristics such as arrival/departure times and drive cycles. Detailed input data specifications are available in the Appendix A.4.

Table 2 exhibits distributed and CMO daily cycle statistics aggregated over all feeders, representing: (i) effective EV cost (i.e., charging cost plus disutility for incomplete charging, minus reserve sale revenues) (ii) social cost (i.e. daily centralized energy generation cost plus reserve provision costs plus EV disutility for incomplete charging upon departure), (iii) centralized generators producer surplus, (iv) daily inelastic demand charges, and (v) transmission rent (inelastic demand charges plus EV energy payments minus payments to the generators for energy).

**Table 2** – Daily financial quantities (\$/day) under different market clearing and information access cases.

	Total EV cost	Social cost	Generator producer surplus	Inelastic demand charges	Transmission rent
D	1636.177	454081.646	258381.123	709465.615	32225.221
$D_A$	1636.177	454081.646	258381.123	709465.615	32225.221
$D_N$	1636.077	454081.685	258381.108	709465.749	32225.320
$D_{N,A}$	1635.574	454081.922	258379.742	709465.334	32225.860
C	1636.177	454081.646	258381.123	709465.615	32225.221
$C_N$	<b>1640.361</b>	<b>454081.015</b>	<b>258378.904</b>	<b>709457.874</b>	<b>32222.518</b>

EV self-scheduling enables strategic behavior to lower effective costs relative to the socially optimal CMO/ $C_N$  equilibrium. EV reliance on load aggregators,  $D_{N,A}$ , strengthens strategic behavior gains. Detailed results for each information availability case are available in Appendix A.4. Average losses are at  $\sim 4.78\%$ , and the transmission rent implied by marginal cost pricing is 7.10% of the total generation costs. DLMP priced conventional demand costs are minimum under CMO/ $C_N$  equilibrium. Network rent is also minimized under the socially optimal CMO/ $C_N$  equilibrium indicating correctly improved asset resilience under optimal market clearing. Finally, as expected by the analytical results of Table 1, CMO/C equilibrium is identical to D and  $D_A$  equilibria.

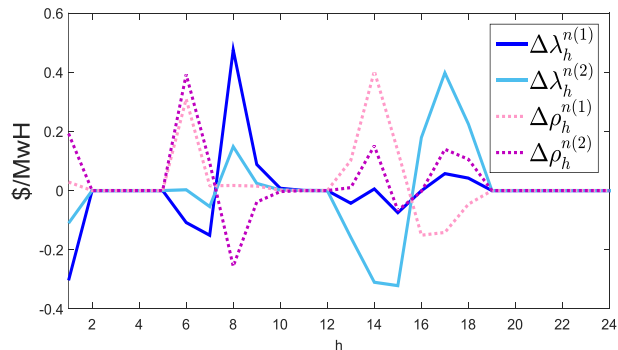
The extra terms in Table 1 demonstrate a clear dependence on the magnitude of the loss factor,  $\beta$ , and the relative size of the flexible load demand and reserve provision. We conducted several numerical experiments described in the first two columns of Table 3 in order to investigate the impact of the factors described above. For expediency, we report the total EV and social cost for cases  $C_N$  and  $D_{N,A}$ .

**Table 3** - Effect of system losses, size of flexible loads on the difference between distributed ( $D_{N,A}$ ) and centralized ( $C_N$ ) solutions.

$\beta \times 10^{-4}$	Flex demand magn.*	Avg. losses %	Tot. EV cost $-D_{N,A}$	Tot. EV cost $-C_N$	Social cost $-D_{N,A}$	Social cost $-C_N$
1	1.4%	4.78	1635.574	1640.361	454081.922	454081.015
2	1.4%	9.04	1909.520	1917.904	482154.259	482151.772
2	1.8%	9.06	2251.865	2272.087	482390.564	482385.672

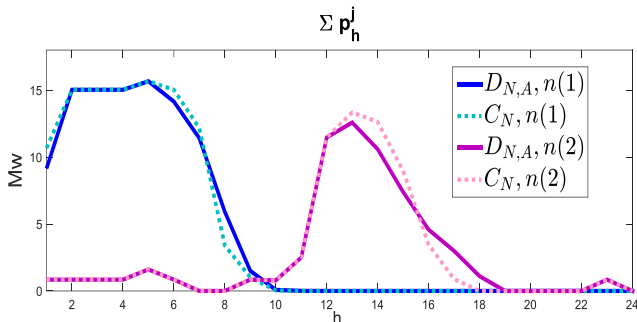
\*Daily EV demand as a percent of daily inelastic demand at feeder 1 & 2.

The results exhibited in Table 3 point in the expected direction: Higher penetration of DERs colluding under a load aggregator and an overloaded distribution network result in the highest deviation from the social optimum. Figure 4 shows feeder specific hourly price and EV consumption differences across market and information access cases  $D_{N,A}$  and  $C_N$ . Figure 4 demonstrates how EV self-scheduling under  $D_{N,A}$  deviates from its  $C_N$  schedule influencing both energy and reserve DLMPs.



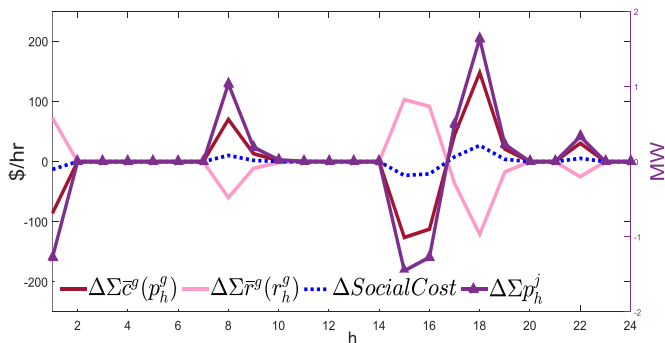
**Figure 4** – Feeder specific Hourly differences in EV energy and reserve schedules and distribution system DLMP<sup>E</sup> and DLMP<sup>R</sup> ( $D_{N,A}$  value -  $C_N$  value).

Figure 5 depicts the hourly differences in the total flexible demand in feeder 1 (residential) and 2 (commercial) across cases  $D_{N,A}$  and  $C_N$ . Residential EV charging mostly takes places after midnight. On the other hand, commercial EV charging demand is higher between hours 10-18.



**Figure 5** - Total EV real power consumption in feeder 1 (residential) and 2 (commercial), for cases  $D_{N,A}$  and  $C_N$ . Commercial demand after hour 19 is zero.

Figure 6 shows the differences in the total hourly cost of real power and reserves produced by centralized generators, the social cost and EV consumption across  $D_{N,A}$  and  $C_N$  ( $D_{N,A}$  value -  $C_N$  value). Note that the social cost (i.e., sum of generation and reserve provision cost) is lower in case  $C_N$  during the hours of lower centralized real power generation, because as it turns out marginal generator energy costs are higher than reserve provision costs. Even though total EV real power consumption, and hence total energy generation, is slightly higher<sup>2</sup> in case  $C_N$  (see Appendix A.4), generation cost is lower than  $D_{N,A}$ ; the CMO achieves under  $C_N$  an overall lower social cost through a different schedule of EV charging.



**Figure 6** - Comparison of total hourly centralized generator energy and reserve costs, social cost, and EV consumption across cases  $D_{N,A}$  and  $C_N$ . ( $D_{N,A}$  value -  $C_N$  value). EV consumption is related to the scale on the right vertical axis depicting MWh.

## VII. CONCLUSION

We have demonstrated that in distributed DAM clearing algorithms, EVs may engage in strategic behavior that become available to them if a future T&D market clears relying on distributed algorithms. The resulting hierarchical game described in sections III and IV can lead to Nash equilibria that may divert from the socially optimal

<sup>2</sup> Although the total energy charged is the same, different charging schedules are associated with different charging efficiencies.

equilibrium under asymmetric access to distribution network information. For all practical intents and purposes, however, there is a credible argument that (i) distributed algorithms are the only practical approach to T&D market clearing, and that (ii) communication constraints suggest that detailed distribution network information cannot be made available to either a single centralized or a multitude of individual DER decision makers, with a possible exception when the distribution utility itself acts as an aggregator empowering DERs to gain market power. And even under these exceptional circumstances, the impact of market power on centralized conventional generation and inelastic conventional demand, is unlikely to be substantial if the distribution system is not allowed to lag seriously behind in maintaining a reasonable capacity level. Nevertheless, detailed empirical studies can determine whether market power issues may arise that are worth imposing additional regulatory constraints such as prohibiting aggregation agreements.

We have also established that the extent to which self-scheduling DERs impact social optimality depends both on their level of penetration and market participation characteristics. EVs can conceivably utilize the functional form of the distribution network losses to influence the DLMPs at their own feeder, and reduce their effective costs relative to the optimal social welfare market schedule. As mentioned, already, the degree to which the social welfare can be unduly influenced appears from our results to be limited. The only case of capacity withholding, can be made for an additional reactive power compensation product, whose DLMP can go be shown to approach zero [14]. In fact, because reactive power compensation may be provided by putting DER power electronics into dual use, there may be no viable economic argument for limiting reactive power compensation capacity. For reactive power compensation, avoiding/regulating load aggregation, or engaging power electronics through the enactment of standards may be a reasonable option. On the other hand, real power and reserve provision through distributed markets, and clearing such markets with distributed algorithms, appears to be a reasonable and fruitful direction for distribution network market creation.

As regards to future work, investigation of distributed algorithms for the realistic and tractable clearing of distribution network markets with high DER penetration, is already attracting increasing attention in the research and practitioner community, and deserves serious further work.

A1. Solutions to the system of differential equations KiBaM.1 and KiBaM.2:

The  $f$  and  $g$  functions are obtained from the solutions of the differential equations KiBaM.1 and 2 as the following:

$$f(b_{h-1}^j, a_{h-1}^j, \mathbf{1}_{h \notin H^j} p_{h-1}^j, \mathbf{1}_{h \in H^j} S_{h-1}^j) = \frac{b_{h-1}^j + a_{h-1}^j}{2} - e^{-2\kappa} \left[ \frac{a_{h-1}^j - b_{h-1}^j}{2} - \frac{u_{h-1}^j}{4\kappa} + \frac{u_{h-1}^j e^{2\kappa}}{4\kappa} \right] - \frac{u_{h-1}^j}{2}$$

$$g(b_{h-1}^j, a_{h-1}^j, \mathbf{1}_{h \notin H^j} p_{h-1}^j, \mathbf{1}_{h \in H^j} S_{h-1}^j) = \frac{b_{h-1}^j + a_{h-1}^j}{2} + e^{-2\kappa} \left[ \frac{a_{h-1}^j - b_{h-1}^j}{2} - \frac{u_{h-1}^j}{4\kappa} + \frac{u_{h-1}^j e^{2\kappa}}{4\kappa} \right] - \frac{u_{h-1}^j}{2}$$

where  $u_{h-1}^j = \mathbf{1}_{h \in H^j} S_{h-1}^j - \mathbf{1}_{h \notin H^j} [(1 - \varepsilon p_{h-1}^j) p_{h-1}^j]$

Noting that the maximum constant charging rate during an hour is the rate that brings the second bucket up to its capacity,  $\bar{b}^j$ , the maximum charging rate function,  $\bar{u}(a_h^j, b_h^j)$ , is written as;

$$\bar{u}_h^j(a_h^j, b_h^j) = 2\kappa \frac{(a_h^j + b_h^j) - e^{-2\kappa} (a_h^j - b_h^j - 2\bar{b}^j)}{e^{-2\kappa} - 2\kappa - 1}$$

A2. Detailed analysis and comparison of equilibrium conditions:

The equilibrium conditions below are derived for a single feeder, single bus network in order to simplify notation. We provide full equilibrium conditions for distributed model case D and centralized model case C<sub>N</sub>, and specify how other informational availability cases influence the equilibrium conditions relative to these two cases. Using the superscript  $f$  to denote the feeder's DLMPs by  $\lambda^f, \rho^f$ , we write the equilibrium conditions of the distributed and the centralized models as follows:

**Equilibrium conditions of EV problem j case D:**

$$\begin{aligned} \mathcal{L}_{EV} = & \sum_h \lambda_h^f p_h^j - \rho_h^f r_h^j + U(a_{h^d}^j + b_{h^d}^j) \\ & - \sum_h v_h^j [b_h^j - f(b_{h-1}^j, a_{h-1}^j, \mathbf{1}_{h \notin H^j} p_{h-1}^j, \mathbf{1}_{h \in H^j} S_{h-1}^j)] \\ & + \sum_h \alpha_h^j [a_h^j - g(b_{h-1}^j, a_{h-1}^j, \mathbf{1}_{h \notin H^j} p_{h-1}^j, \mathbf{1}_{h \in H^j} S_{h-1}^j)] \\ & + \sum_{g,h} \zeta_h^j [p_h^j - \min\{\bar{P}, \bar{u}_h(a_h^j, b_h^j)\} + \varepsilon (\bar{u}_h(a_h^j, b_h^j))^2] \\ & + \sum_{g,h} \delta_h^j [r_h^j - \min\{p_h^j, \bar{P} - p_h^j, 0.8 \bar{u}_h(a_h^j, b_h^j)\}] \\ & + \sum_h \varrho_h^{j,a} [a_h^j - \bar{a}^j] \\ & + \sum_h \varrho_h^{j,b} [b_h^j - \bar{b}^j] \end{aligned}$$

$$\begin{aligned} \partial \mathcal{L}_{EV} / \partial p_h^j &= \lambda_h^f + v_{h+1}^j \partial f(b_h^j, a_h^j, \mathbf{1}_{h \notin H^j} p_h^j, \mathbf{1}_{h \in H^j} S_h^j) / \partial p_h^j \\ & - \alpha_{h+1}^j \partial g(b_h^j, a_h^j, \mathbf{1}_{h \notin H^j} p_h^j, \mathbf{1}_{h \in H^j} S_h^j) / \partial p_h^j + \zeta_h^j - \delta_h^j = 0 \\ \partial \mathcal{L}_{EV} / \partial r_h^j &= -\rho_h^f + \delta_h^j = 0 \end{aligned}$$

**Equilibrium conditions of the TISO problem:**

$$\begin{aligned} \mathcal{L}_{TISO} = & \sum_{g,h} [\bar{c}^g(p_h^g) + \bar{r}^g(r_h^g)] \\ & - \sum_h \lambda_h [\sum_g p_h^g - \sum_j p_h^j - d_h - 0.5\beta(\sum_j p_h^j + d_h)^2] \\ & + \sum_h \rho_h [R_h - \sum_g r_h^g - \sum_j (1 + \beta(\sum_j p_h^j + d_h)) r_h^j] \\ & + \sum_{g,h} \zeta_h^g [-p_h^g + r_h^g + \underline{g}] \\ & + \sum_{g,h} \xi_h^g [p_h^g + r_h^g - \bar{g}] \end{aligned}$$

$$\begin{aligned} \partial \mathcal{L}_{TISO} / \partial p_h^g &= \partial \bar{c}(p_h^g) / \partial p_h^g - \lambda_h - \zeta_h^g + \xi_h^g = 0 \\ \partial \mathcal{L}_{TISO} / \partial r_h^g &= \partial \bar{r}(r_h^g) / \partial r_h^g - \rho_h + \zeta_h^g + \xi_h^g = 0 \end{aligned}$$

Note that the intertemporal dynamics coupling EV charging decisions,  $p_h^j$ , across hours are captured in equilibrium condition  $\partial \mathcal{L}_{EV} / \partial p_h^j = 0$  by the presence of dual variable  $v_{h+1}^j$  related to hour  $h+1$ .

The equilibrium conditions of the CMO clearing problem under full distribution network information access, C<sub>N</sub>, are derived next.

### Equilibrium conditions of Case C<sub>N</sub>:

$$\begin{aligned}
\mathcal{L}_{CMO} = & \sum_{g,h} \left[ \bar{c}^g(p_h^g) + \bar{r}^g(r_h^g) \right] + U(a_{h^d}^j + b_{h^d}^j) \\
& - \sum_h \lambda_h \left[ \sum_g p_h^g - \sum_j p_h^j - d_h - \frac{\beta}{2} (\sum_j p_h^j + d_h)^2 \right] \\
& + \sum_h \rho_h \left[ R_h - \sum_g r_h^g - \sum_j (1 + \beta (\sum_j p_h^j + d_h)) r_h^j \right] \\
& + \sum_{g,h} \zeta_h^g \left[ -p_h^g + r_h^g + \underline{g} \right] \\
& + \sum_{g,h} \xi_h^g \left[ p_h^g + r_h^g - \bar{g} \right] \\
& - \sum_h \nu_h^j \left[ b_h^j - f(b_{h-1}^j, a_{h-1}^j, \mathbf{1}_{h \notin H^j} p_{h-1}^j, \mathbf{1}_{h \in H^j} S_{h-1}^j) \right] \\
& + \sum_h \alpha_h^j \left[ a_h^j - g(b_{h-1}^j, a_{h-1}^j, \mathbf{1}_{h \notin H^j} p_{h-1}^j, \mathbf{1}_{h \in H^j} S_{h-1}^j) \right] \\
& + \sum_{g,h} \zeta_h^j \left[ p_h^j - \min \{ \bar{P}, \bar{u}_h(a_h^j, b_h^j) \} + \varepsilon (\bar{u}_h(a_h^j, b_h^j))^2 \right] \\
& + \sum_{g,h} \delta_h^j \left[ r_h^j - \min \{ p_h^j, \bar{P} - p_h^j, 0.8 \bar{u}_h(a_h^j, b_h^j) \} \right] \\
& + \sum_h \mathcal{G}_h^{j,a} \left[ a_h^j - \bar{a}^j \right] \\
& + \sum_h \mathcal{G}_h^{j,b} \left[ b_h^j - \bar{b}^j \right]
\end{aligned}$$

$$\begin{aligned}
\partial \mathcal{L}_{CMO} / \partial p_h^j = & \lambda_h [1 + \beta (\sum_j p_h^j + d_h)] - \rho_h \beta \sum_j r_h^j \\
& + \nu_{h+1}^j \frac{\partial f(b_h^j, a_h^j, \mathbf{1}_{h \notin H^j} p_h^j, \mathbf{1}_{h \in H^j} S_h^j)}{\partial p_h^j} \\
& - \alpha_{h+1}^j \frac{\partial g(b_h^j, a_h^j, \mathbf{1}_{h \notin H^j} p_h^j, \mathbf{1}_{h \in H^j} S_h^j)}{\partial p_h^j} + \zeta_h^j - \delta_h^j = 0
\end{aligned}$$

$$\partial \mathcal{L}_{CMO} / \partial r_h^j = -\rho_h [1 + \beta (\sum_j p_h^j + d_h)] + \delta_h^j = 0$$

$$\partial \mathcal{L}_{CMO} / \partial p_h^g = \partial \bar{c}(p_h^g) / \partial p_h^g - \lambda_h - \zeta_h^g + \xi_h^g = 0$$

$$\partial \mathcal{L}_{CMO} / \partial r_h^g = \partial \bar{r}(r_h^g) / \partial r_h^g - \rho_h + \zeta_h^g + \xi_h^g = 0$$

The bold term in the gradient  $\partial \mathcal{L}_{CMO} / \partial p_h^j$  represents the optimality mismatch term when compared to the gradient  $\partial \mathcal{L}_{EV} / \partial p_h^j$  in the distributed model case D.

Lagrangian and Optimality conditions for **case D<sub>N</sub>** differ as follows; after convergence, the gradient  $\partial \mathcal{L}_{EV} / \partial p_h^j$  in **case D<sub>N</sub>** becomes:

$$\begin{aligned}
\partial \mathcal{L}_{EV} / \partial p_h^j = & \lambda_h [1 + \beta (p_h^j + \ell_h^j)] + \beta \lambda_h p_h^j - \beta \rho_h r_h^j \\
& + \nu_{h+1}^j \frac{\partial f(b_h^j, a_h^j, \mathbf{1}_{h \notin H^j} p_h^j, \mathbf{1}_{h \in H^j} S_h^j)}{\partial p_h^j} \\
& - \alpha_{h+1}^j \frac{\partial g(b_h^j, a_h^j, \mathbf{1}_{h \notin H^j} p_h^j, \mathbf{1}_{h \in H^j} S_h^j)}{\partial p_h^j} + \zeta_h^j - \delta_h^j = 0.
\end{aligned}$$

Note that in case D<sub>N</sub>, the DLMP is written explicitly as the product of bus LMP and the marginal loss function, where the marginal loss is a function of the individual and the complementary EV consumption. The bold terms in the equilibrium condition above show the terms that do not appear in case D. Notice that even in the absence of reserve trading, the difference  $\beta \lambda_h p_h^j$  persists.

On the other hand, the objective function for **case D<sub>N,A</sub>** becomes,

$$\sum_{j,h} [1 + \beta (\sum_j p_h^j + d_h)] (\lambda_h p_h^j - \rho_h r_h^j) + U(a_{h^d}^j + b_{h^d}^j)$$

Hence,

$$\begin{aligned}
\partial \mathcal{L}_{EV} / \partial p_h^j = & \lambda_h [1 + \beta (\sum_j p_h^j + d_h)] \\
& + \lambda_h \beta \sum_j p_h^j - \rho_h \beta \sum_j r_h^j \\
& + \nu_{h+1}^j \frac{\partial f(b_h^j, a_h^j, \mathbf{1}_{h \notin H^j} p_h^j, \mathbf{1}_{h \in H^j} S_h^j)}{\partial p_h^j} \\
& - \alpha_{h+1}^j \frac{\partial g(b_h^j, a_h^j, \mathbf{1}_{h \notin H^j} p_h^j, \mathbf{1}_{h \in H^j} S_h^j)}{\partial p_h^j} + \zeta_h^j - \delta_h^j = 0
\end{aligned}$$

Analysis of the above conditions indicate equilibrium mismatches between certain cases of the distributed and the centralized models, which are summarized in Table 1.

### A.3 Convergence of the Distributed Algorithm

At each iteration  $k+1$  of the distributed algorithm, individual EVs or Load Aggregators (depending on the case) receive updated DLMP<sup>E</sup> and DLMP<sup>R</sup> prices,  $\hat{\lambda}_h^{k+1}, \hat{\rho}_h^{k+1}$  from the TISO. The TISO updates last iteration's prices by an increment that is proportional to but generally smaller than the distance of last iteration's prices from the current iteration's ex post marginal-cost-based prices. A step size that is less than 1 is used in-order to avoid oscillatory behavior. More specifically, the step size depends on the sign of the change in the EV problem's schedule of iteration  $k+1$ , relative to iteration  $k$ . The algorithm adopts a smaller, hence more conservative, step sizes when the change is negative indicating an overshoot. On the other hand, if there is no direction change in the last few iterations, step size is increased by a pre-determined factor. The adaptive price update algorithm employed is described below.

**Initialization** (start from  $k=0$ ):

$$\varphi_h^{\lambda,k} = \varphi_0^\lambda, \quad \varphi_h^{\rho,k} = \varphi_0^\rho \text{ for case D}_N$$

$$\varphi_h^{\lambda^{n(i),k}} = \varphi_0^{\lambda^{n(i)}}, \quad \varphi_h^{\rho^{n(i),k}} = \varphi_0^{\rho^{n(i)}} \text{ for case D,}$$

Choose  $\underline{\alpha} \in (0,1)$  and  $\bar{\alpha} > 1$

**Step 1.** Solve EV problems and find

$$p_h^{j,k+1}, r_h^{j,k+1}, m_h^{n(i),k+1},$$

**Step 2.** Solve ISO problem and find  $\lambda_h^{k+1}, \rho_h^{k+1}$  and  $\lambda_h^{n(i),k+1}, \rho_h^{n(i),k+1}$

**Step 3 Compute**

$$\Delta \lambda_h^{k+1} = \hat{\lambda}_h^k - \lambda_h^{k+1}, \Delta \rho_h^{k+1} = \hat{\rho}_h^k - \rho_h^{k+1}$$

$$\Delta \lambda_h^{n(i),k+1} = \hat{\lambda}_h^{n(i),k} - \lambda_h^{n(i),k+1}, \Delta \rho_h^{n(i),k+1} = \hat{\rho}_h^{n(i),k} - \rho_h^{n(i),k+1}$$

**If**  $\text{sgn}(\Delta \lambda_h^{k+1} \Delta \lambda_h^k) = -1$  **then**

$$\varphi_h^{\lambda,k+1} = \min \{ \varphi_0^\lambda, \alpha \varphi_h^{\lambda,k} \}$$

**Else**  $\varphi_h^\lambda = \min \{ \varphi_0^\lambda, \bar{\alpha} \varphi_h^{\lambda,k} \}$  **endif.**

**Similarly repeat if-then of step 3 to find**

$$\rho_h^{k+1}, \lambda_h^{n(i),k+1}, \rho_h^{n(i),k+1}$$

**Step 4 Update**

$$\hat{\lambda}_h^{k+1} := \hat{\lambda}_h^k - \varphi_h^{\lambda,k} \Delta \lambda_h^{k+1}; \hat{\rho}_h^{k+1} := \hat{\rho}_h^k - \varphi_h^{\rho,k} \Delta \rho_h^{k+1}$$

For case DN, and similarly  $\hat{\lambda}_h^{n(i),k+1}, \hat{\rho}_h^{n(i),k+1}$  for case D.

**If**  $\sum_h (\hat{\lambda}_h^{k+1} - \lambda_h^{k+1})^2 \geq \varepsilon$  **then**

$k \leftarrow k+1$  and Go to **Step 1.** **endif.**

Convergence of  $\hat{\lambda}_h^k$  to  $\lambda_h^k$  as  $k$  increases is shown for case DN,A, for a selected representative hour in Figure A.3.1. Total flexible demand is plotted against the right axis showing MWh.

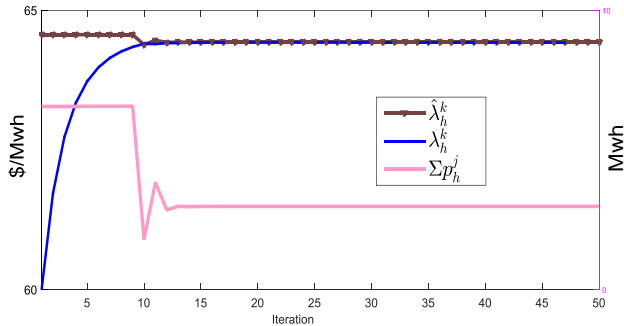


**Figure A.3.1** - Convergence of TISO provider energy LMP estimate for a selected hour to the actual LMP in case DN,A. The evolution of total EV consumption is also plotted against the the right axis showing MWh.

Figure A.3.2 shows the  $\text{LMP}^E$  convergence metric in case DN,A by plotting the total sum of squares difference over all hours  $\sum_h (\hat{\lambda}_h^k - \lambda_h^k)^2$ . Convergence is shown for two step size update algorithms; (i) the aforementioned direction dependent adaptive step size and (ii) a simpler step size diminishing with iterations according to  $\sqrt{1/k}$ .

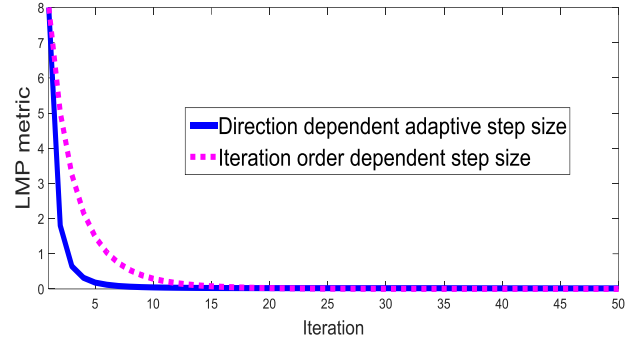


**Figure A.3.2** –  $\text{LMP}^E$  metric across iterations for case DN,A. The convergence is shown for two step size update algorithms. The reserve  $\text{LMP}^R$  metric follows a similar trend.

As stated in the Adaptive Step Size algorithm, in cases D and DA (i.e., in the absence of network information access), the convergence metric is based on the DLMPs, rather than LMPs.

#### A.4 Numerical Experiment Details

Table A.4.1-2 below shows the detailed input data used in the experiments.

**Table A.4.1** – EV group data

EV group	Number in group	Arrival time		Departure time	
		Feeder 1	Feeder 2	Feeder 1	Feeder 2
1	690	21	10	7	17
2	690	21	11	7	18
3	1380	23	12	9	21
4	172	7	0	22	6
5	345	0	14	12	23
6	172	23	8	6	19

**Table A.4.2** – Inelastic demand and generation data

24 hour inelastic demand (MWh)	24 hour system reserve requirement (MWh)	Range of hourly demand (MWh)	Hourly generation capacity (MW)
8760	560	215-522	700

In the following tables, we present the details of the aggregate results presented in Table 2. Table A.4.3 shows the absolute differences between the benchmark socially optimal case CN and the rest of the centralized and distributed information availability cases.

**Table A.4.3** - Social optima deviation of each market participant from the social welfare maximizing  $C_N$

	Total EV cost	Social cost	Generator producer surplus	Inelastic demand charges	Transmission rent
$C_N$ -D	4.184	-0.631	-2.219	-7.741	-2.703
$C_N$ -D <sub>A</sub>	4.184	-0.631	-2.219	-7.741	-2.703
$C_N$ -D <sub>N</sub>	4.284	-0.67	-2.204	-7.875	-2.802
$C_N$ -D <sub>N,A</sub>	4.787	-0.907	-0.838	-7.46	-3.342
$C_N$ -C	4.184	-0.631	-2.219	-7.741	-2.703
<b><math>C_N</math></b>	<b>1640.361</b>	<b>454081.015</b>	<b>258378.904</b>	<b>709457.874</b>	<b>32222.518</b>

Table A.4.4 shows the components of the social cost and total generator surplus presented in Table 2. Note that even though the reserve provision cost is highest in the welfare maximizing case  $C_N$ , it is dominated by the lower real power generation cost to yield a lowest social cost.

**Table A.4.4** - Total generator real power and reserve cost/surplus

	Generator Real power generation cost	Generator Reserve provision cost	Generator Profit from real power	Generator Profit from reserve provision
D	430597.628	23484.018	257000.788	1380.335
D <sub>A</sub>	430597.628	23484.018	257000.788	1380.335
D <sub>N</sub>	430597.784	23483.901	257000.946	1380.161
D <sub>N,A</sub>	430598.730	23483.192	257000.760	1378.982
C	430597.628	23484.018	257000.788	1380.33
<b><math>C_N</math></b>	<b>430593.610</b>	<b>23487.405</b>	<b>256993.108</b>	<b>1385.796</b>

The total amount of real power consumed/reserves provided by flexible loads is shown in Table A.4.5 below for all information availability cases.

**Table A.4.5** - Total flexible consumption/reserve provision and conventional generation/reserve provision across all cases

	EV real power consumption (MW/day)	EV Reserve provision (MW/day)	Gen. real power generation (MW/day)	Gen. reserve provision (MW/day)
D	140.841	139.006	9326.925	405.512
D <sub>N</sub>	140.839	139.004	9326.923	405.514
D <sub>N,A</sub>	140.833	138.998	9326.921	405.519
<b><math>C_N</math></b>	<b>140.880</b>	<b>139.045</b>	<b>9326.947</b>	<b>405.466</b>

## REFERENCES

- [1] P. Richardson, D. Flynn, and A. Keane, "Optimal charging of electric vehicles in low-voltage distribution systems," *IEEE TPS* 2012.
- [2] M. A. Lopez, J. A. Aguado, S. Torre, and M. Figuerola, "Optimization-based market-clearing procedure with EVs aggregator participation," in *ISGT EUROPE, 2013 4th IEEE/PES*, IEEE, 2014.
- [3] D. Wu, D. C. Aliprantis, and L. Ying, "Load scheduling and dispatch for Aggregators of plug-in electric vehicles," *IEEE TSG*, 2012A.
- [4] D. Dominguez-Garcia, S. T. Cady, and C. N. Hadjicostis, "Decentralized Optimal Dispatch of Distributed Energy Resources," in *51st IEEE Conference on Decision and Control*, IEEE, 2012.
- [5] C. Le Floch, F. Belletti, S. Saxena, A. M. Bayen, and S. Moura, "Distributed Optimal Charging of Electric Vehicles for Demand Response and Load Shaping," in *2015 IEEE 54th CDC*, IEEE, 2015.
- [6] L. Gan, U. Topcu, and S. H. Low, "Optimal decentralized protocol for electric vehicle charging," *IEEE TPS*, vol. 28, no. 2, pp. 940–951, May 2013.
- [7] Z. Ma, D. S. Callaway, and I. A. Hiskens, "Decentralized charging control of large populations of plug-in electric vehicles," *IEEE Transactions on Control Systems Technology*, vol. 21, no. 1, pp. 67–78, Jan. 2013.
- [8] E. Ntakou and M. Caramanis, "Distribution network electricity market clearing: Parallelized PMP algorithms with minimal coordination," in *53rd IEEE Conference on Decision and Control*, IEEE, 2014
- [9] M. G. Vaya, S. Grammatico, G. Andersson, and J. Lygeros, "On the price of being selfish in large populations of plug-in electric vehicles," *2015 CDC*
- [10] M. Caramanis and J. M. Foster, "Uniform and complex bids for demand response and wind generation scheduling in multi-period linked transmission and distribution markets," in *2011 50th IEEE CDC and ECC*
- [11] M. Caramanis, E. Goldis, P. Ruiz, and A. Rudkevich, "Power market reform in the presence of flexible schedulable distributed loads. New bid rules, equilibrium and tractability issues," in *Communication, Control, and Computing (Allerton), 2012 50th Annual Allerton Conference*, IEEE, 2012.
- [12] E. M. Krieger and C. B. Arnold, "Effects of undercharge and internal loss on the rate dependence of battery charge storage efficiency," *Journal of Power Sources*, vol. 210, pp. 286–291, Jul. 2012.
- [13] S. J. Moura, J. L. Stein, and H. K. Fathy, "Battery-health conscious power management in plug-in hybrid electric vehicles via Electrochemical modeling and stochastic control," *IEEE Transactions on Control Systems Technology*, vol. 21, no. 3, pp. 679–694, May 2013
- [14] M. Caramanis, E. Ntakou, W. Hogan, A. Chakraborty and J. Schoene, "Co-Optimization of Power and Reserves in Dynamic T&D Power Markets with Non-Dispatchable Renewable Generation and Distributed Energy Resources" *Proceedings of IEEE*, Vol. 104, No. 4, pp. 807-836, April 2016
- [15] J. M. Foster, M. C. Caramanis "Optimal Power Market Participation of Plug-In Electric Vehicles Pooled by Distribution Feeder" *IEEE TPS* 2013.
- [16] K. Arrow, and G. Debreu, Existence of an Equilibrium for a Competitive Economy, 1954
- [17] J. F. Manwell and J. G. Mcgowan, "Lead acid battery storage model for hybrid energy systems," *Solar Energy*, vol. 50, no. 5, pp. 399–405, 1993.
- [18] B. Ghahesifard, T. Basar, and A. D. Dominguez-Garcia, "Price-based distributed control for networked plug-in electric vehicles," *2013 ACC*, 2013.
- [19] J. F. Marley, D. K. Molzahn, and I. A. Hiskens, "Solving Multiperiod OPF problems using an AC-QP algorithm Initialized with an SOCP relaxation," *IEEE TPS*, pp. 1–1, 2016.
- [20] Rosen, J.B., Existence and uniqueness of equilibrium points for concave n-person games. *Econometrica*, Vol. 33 (3) pp. 520-534, 1965.
- [21] L. Deori, K. Margellos, and M. Prandini. On decentralized convex optimization in a multi-agent setting with separable constraints and its application to optimal charging of electric vehicles. *IEEE CDC*, 2016.